Expanded View Figures

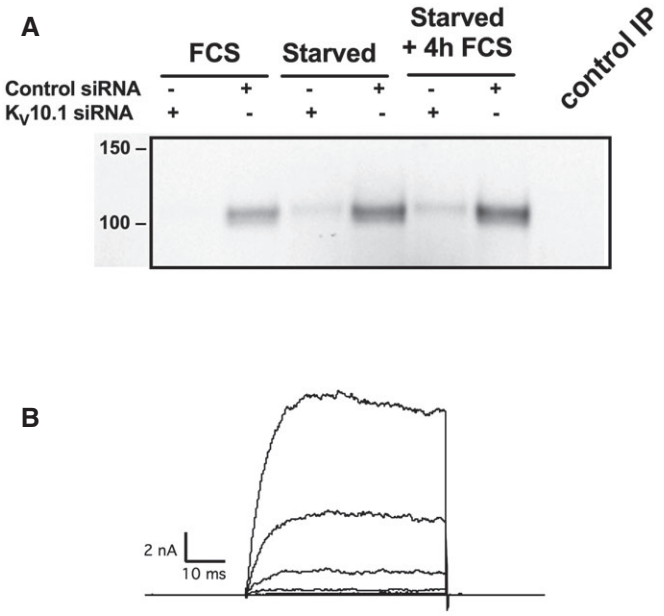

Figure EV1. Expression of Kv10.1 in hTERT-RPE1 cells and efficacy of siRNA.

A By real-time PCR and Western blot, we tested the expression of K_V10.1 in hTERTRPE1 cells and found that K_V10.1 expression is almost as abundant as in brain at the RNA level, and a clear protein band, consistent with K_V10.1, could be detected by Western blot after immunoprecipitation. Immunoprecipitation and Western blotting were performed with antibodies recognizing different parts of the protein, reinforcing the idea that the detected bands indeed correspond to K_V10.1. Additionally, siRNA against K_V10.1 strongly reduced the signal at both the RNA (by a factor of 0.143 ± 0.022 by real-time RT–PCR) and protein level, in cells actively proliferating, serum-starved, or after reintroduction of serum for 4 h. In all cases, immunoprecipitation was required to detect K_V10.1 bands, indicating low abundance of the protein, despite the relatively high concentration of mRNA (in the same range as detected in total human brain).

B In agreement with this, hTERT-RPE1 cells gave only an outward current at very depolarized potentials whose features were not compatible with K_V10.1, indicating that the protein is either scarce (as inferred from immunoprecipitation experiments) or not functional at the plasma membrane. The figure shows a representative example of the appearance of current traces at different stimulus potentials (from −80 to + 140 mV). Only the three most intense depolarizing stimuli induce voltage-gated currents (+ 100, + 120, and + 140 mV).

Source data are available online for this figure.

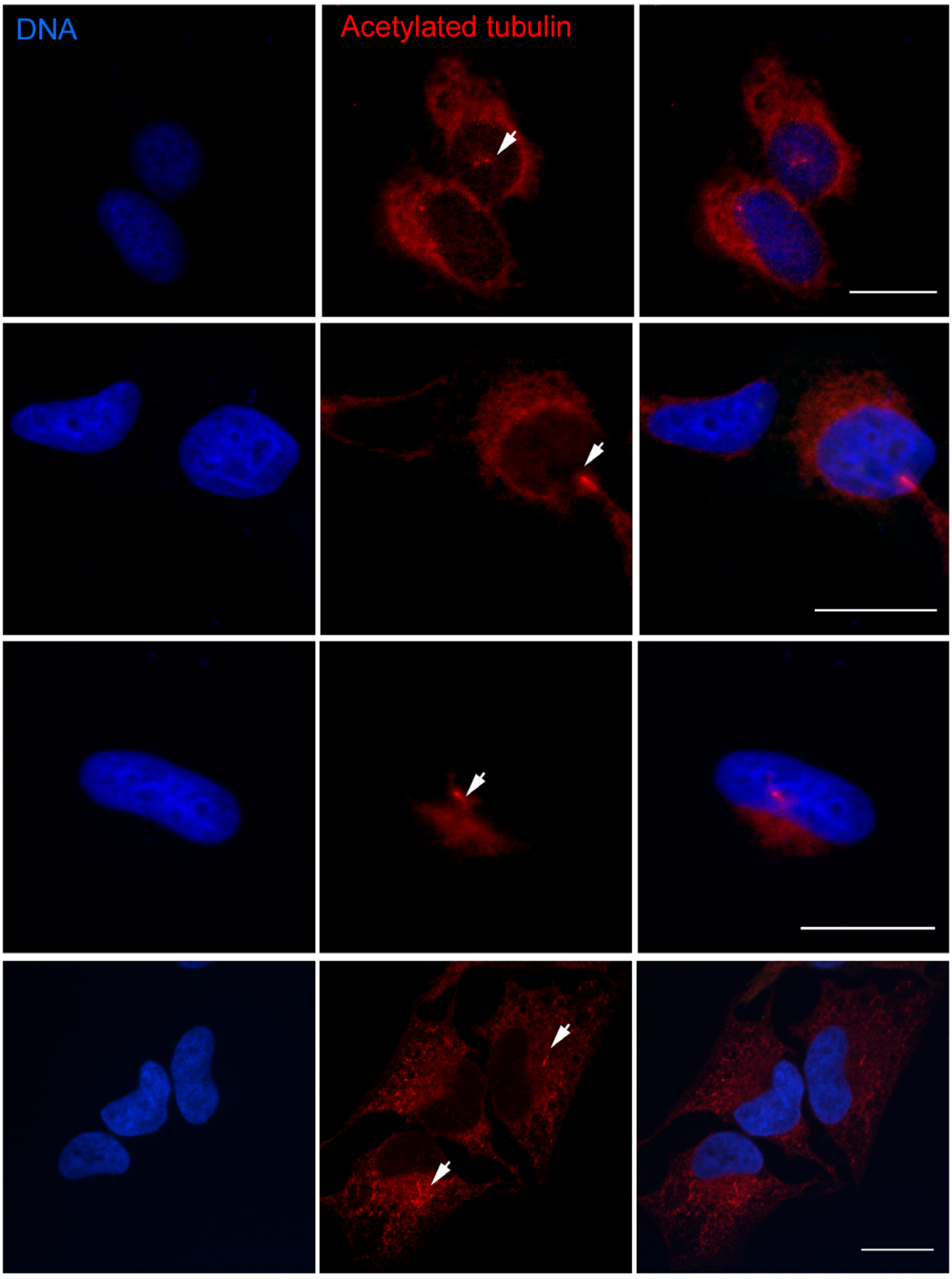

Figure EV2. Primary cilia in HeLa cells treated with siRNA against K_V10.1.
Non-ciliated HeLa cells were treated with siRNA against K_V10.1, serum-starved for 48 h, and stained with anti-acetylated α-tubulin antibody and Draq5 (for DNA) to reveal the presence of primary cilia (arrows). Scale bar: 30 μm.

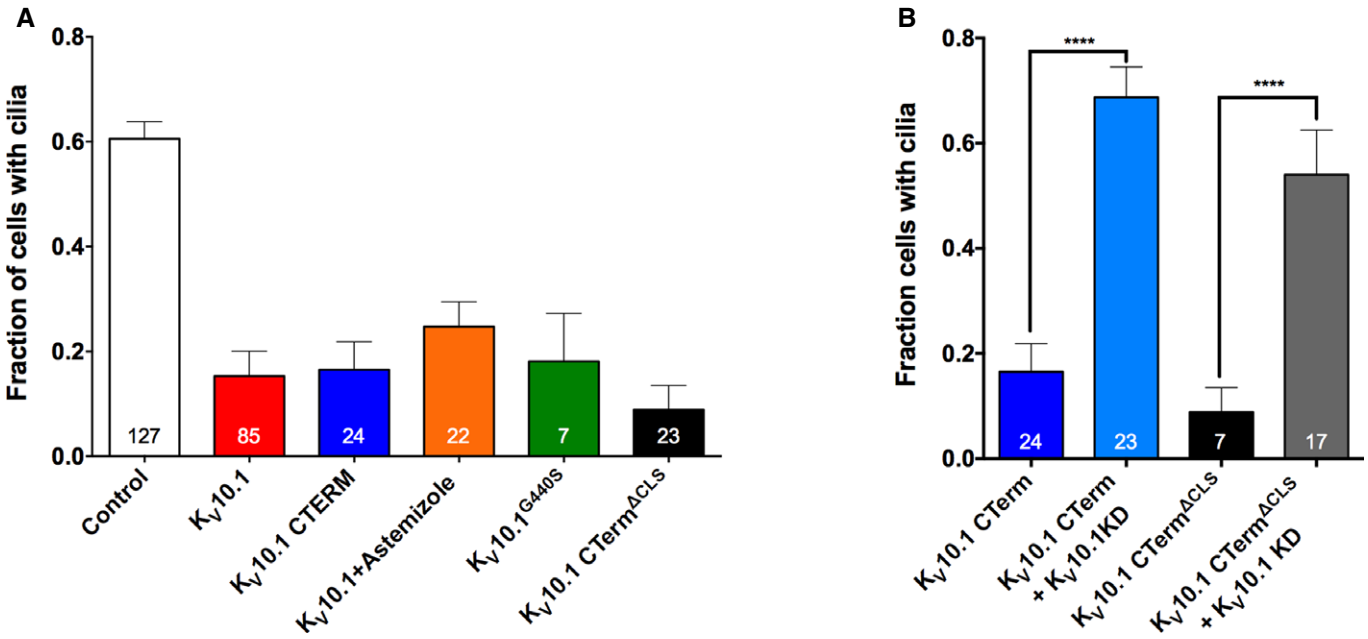

Figure EV3. Dual role of K_V10.1 on ciliary disassembly and maintenance of deciliation.

A K_V10.1 overexpression reduced the frequency of ciliated cells not only in cells reentering the cell cycle, but also in serum-starved cells. Under these conditions, reduction of the number of ciliated cells was not dependent on potassium permeation and occurred when only the intracellular C-terminus was transfected, when K^+ permeation was inhibited by 10 μM astemizole, or when a non-permeant channel (G440S) was used. This phenomenon was also not dependent on the presence of a CLS.

B When measuring ciliary disassembly (4-h serum reintroduction after 24-h serum starvation), the action of the C-terminus of K_V10.1 (with or without CLS) was counteracted by knockdown of endogenous channels by siRNA. Because the siRNA is directed against transmembrane regions of the channel, it is not expected to affect the abundance of the transfected construct. Taken together, these results indicate that the actions of K_V10.1 expression on primary cilia are mechanistically twofold. On one hand, in cells that are not ciliated, K_V10.1 inhibits reciliation, probably in a similar way as already described for other proteins (like pVHL [60]). Potassium permeation through the channel is not required to maintain cells deciliated, because a non-permeating mutant (or pharmacological inhibition of permeation) and even the C-terminus of K_V10.1 alone, which shows no membrane-spanning domains, all inhibit ciliogenesis in serum-starved cells. Mutants where the CLS has been deleted are also equally efficient in maintaining deciliation. Probably for this reason, the difference in ciliation between primary cells from K_V10.1 knockout and wild-type mice was much more evident when serum was withdrawn, cells allowed to produce cilia for 24 h, and then, serum was reintroduced for 4 h (Fig 3A) to induce deciliation.

Data information: Data are presented as mean ± SEM. ****$P < 0.0001$ (two-way ANOVA).

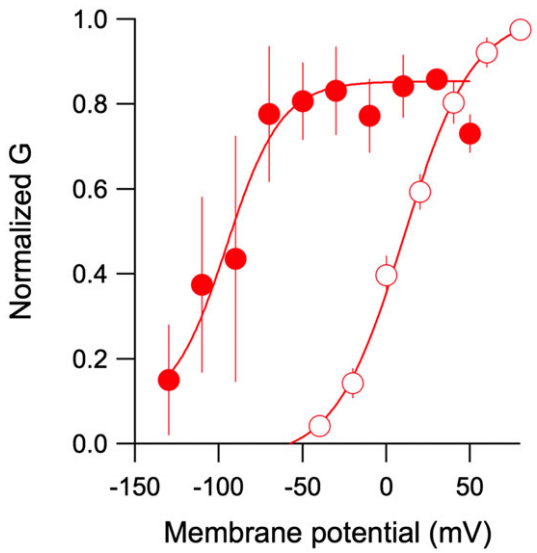

Figure EV4. K_V10.1L352V channels show a dramatic shift of their voltage dependence to hyperpolarized potentials.

Currents were studied in HEK cells transfected with the mutant channel [24] by whole-cell patch clamp. K_V10.1L352V channels (red solid circles) activate at potentials approximately 100 mV more negative than the wild-type channel (open circles). Conductance-voltage plots were constructed using the amplitude of the tail current at −150 mV after a 500-ms depolarizing pulse ranging from −130 to + 50 mV with 20-mV intervals. Experiments were performed using an EPC9 amplifier (HEKA electronics). Patch pipettes had resistances of 2–3 MΩ. The internal solution contained 100 mM KCl, 45 mM N-methyl-D-glucamine, 5 mM 1,2-bis(*O*-aminophenoxy)ethane-N,N,N′,N′-tetraacetic acid (BAPTA), 5 mM EGTA, 1 mM $MgCl_2$, and 10 mM HEPES pH 7.4. The external solution contained 100 mM NaCl, 62.5 mM KCl, 2 mM $CaCl_2$, 1 mM $MgCl_2$, 8 mM glucose, 10 mM HEPES pH 7.4. Series resistance was compensated to 85%.

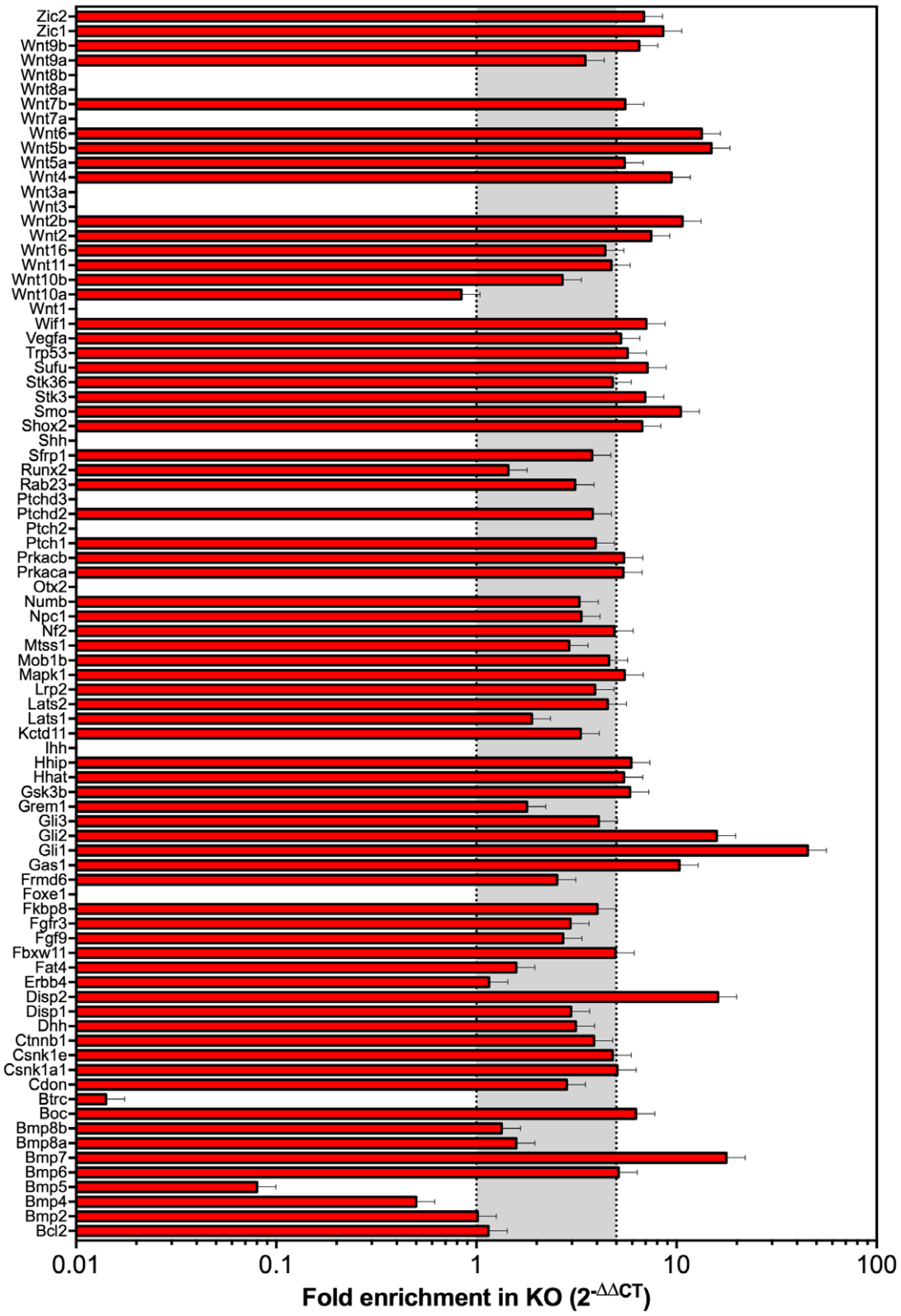

Figure EV5. mRNA enrichment in K_V10.1 KO MEFs of genes related to the SHH pathway.
The RT2Profiler PCR Array Mouse Hedgehog Signaling Pathway (PAMM-078ZG, Qiagen SAB) was used to study the prevalence of mRNAs of 84 SHH-related genes (and 5 housekeeping genes). The gray area indicates up to fivefold enrichment. Relevant genes such as *Gli1* and *Gli2* showed over 10-fold more abundance in MEFs from knockout mice.

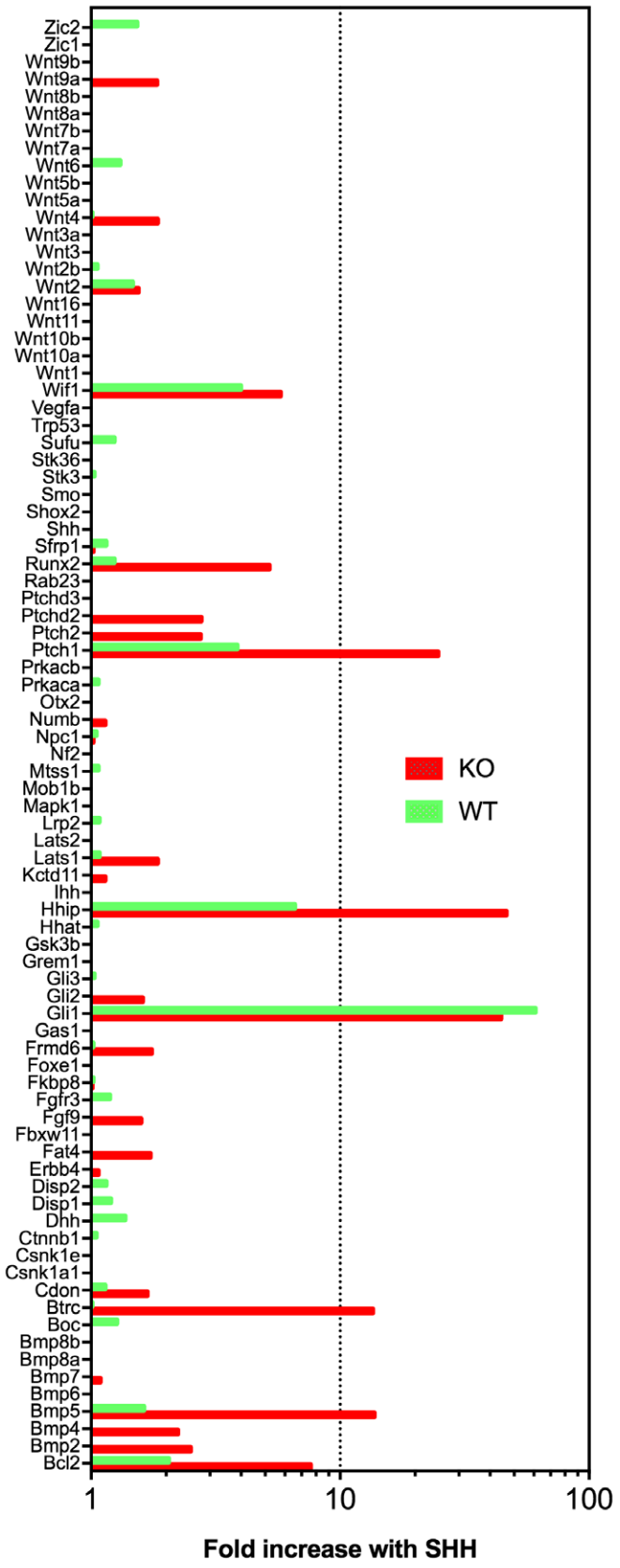

Figure EV6. SHH induced more intense changes in K_V10.1 knockout MEFs.

The abundance of genes was determined as in Fig EV5 after SHH stimulation (4 h after 24-h serum starvation; see Materials and Methods). Both types of MEFs (wild-type and K_V10.1 knockout) responded qualitatively similar to the treatment, but the response for several genes (especially *Hhip* and *Ptch1*) was more intense in the knockout MEFs.